JOURNAL OF Applied Polymer SCIENCE

Analysis of the Dielectric Spectroscopy of an Epoxy-ZnO Nanocomposite Using the Universal Relaxation Law

Wenhu Yang, Ran Yi, Sisi Hui, Yang Xu, Xiaolong Cao
State Key Laboratory of Power Equipment and Electrical Insulation, Xi'an Jiaotong University, Xi'an 710049, China
Correspondence to: W. Yang (E-mail: tiger-y@163.com)

ABSTRACT: There is currently no unified theory that explains the role of nanofillers in polymeric insulation. Consequently, different methods such as dielectric spectroscopy analysis are used to understand this role. The existence of a strong interaction between nanoparticles and a polymer is widely accepted. However, the interaction between dipoles has been taken into consideration in Jonscher's Universal Relaxation Law (URL) but not in the Debye theory. Hence, the URL was used in this article as a method to analyze the spectra of epoxy-ZnO nanocomposites and to try to determine the nanoeffect mechanism. At 160°C above T_g (116°C), the typical phenomenon of low-frequency dispersion occurs in the epoxy-ZnO nanocomposites, and with filler loading increased up to 5 wt %, the value of n (calculated from the ε_r'' spectrum of the nanocomposites) increases both at high and low frequencies. This result indicates that higher loadings correspond to lower dielectric losses changing per radian. Moreover, the decrease in quasi-direction conduction indicates that the gross dielectric losses of the nanocomposites are also less than pure epoxy resin (EP) at low frequencies. This finding may be attributed to the strong bonding between the nanofillers and the EP, which limits the movement of some macromolecular chains. The URL provides an analytical method for determining the mechanism of the effect of nanofillers on polymers.
© 2012 Wiley Periodicals, Inc. J. Appl. Polym. Sci. 000: 000–000, 2012

KEYWORDS: nanocomposite; dielectric properties; interfaces; differential scanning calorimetry (DSC)

Received 17 September 2011; accepted 14 March 2012; published online 00 Month 2012
DOI: 10.1002/app.37696

INTRODUCTION

Polymer nanocomposites possess promisingly high performances as engineering materials.[1,2] Studies have indicated that even a small fraction of inorganic nanofillers added to a polymer improves its dielectric properties. Such improved properties include resistivity, breakdown strength, resistance to partial discharge, and so on.[2–4] In 1994, Lewis[5] proposed for the first time the concept of nanocomposites as dielectric materials. Since then, electrical engineering researchers have exerted extensive efforts to determine the reason for nanoparticles being able to improve the dielectric properties of a polymer. Lewis[6] and Nelson and coworkers[7] proposed that the interface between nanofillers and a polymer plays an important role in determining material properties. Tanaka[1,8] established a multishell model to explain the changes in the polymer dielectric properties on the addition of nanofillers. In his model, interaction zones were divided three layers and a superimposed Gouy–Chapman diffuse layer. However, issues concerning the dielectric nature of the interaction zone and its composition are not yet completely known until now.[9]

Numerous analytical methods are used to investigate the interaction of nanofillers with polymer matrices. The methods include dielectric spectroscopy, thermally stimulated currents, infrared spectroscopy, space charge measurement, and so on.[7,10–12] Dielectric spectroscopy, which is sensitive to a variety of relaxations, is a powerful experimental method for studying the dynamic behavior of polymer composites.[13] Indeed, the spectra of nanocomposites have been studied by many researchers. Zhang and Stevens[14] added nanoalumina to polyethylene and epoxy resin (EP). They found that the dielectric spectra of EP and epoxy nanocomposite were different when they contained 0.4% absorbed water, which was not observed under dry conditions. In polyethylene nanocomposites with residual water, a dielectric loss peak produced by the incorporation of nanoalumina also exhibits the same type of unusual behavior as that observed in undried epoxy nanodielectrics. The authors believe that this behavior arises from the interplay between interfacial water mobility and bonding, rather than from the host polymer molecules. Zou et al.[15] also studied the effect of water absorption on the dielectric properties of epoxy materials. They observed that the low-frequency dielectric spectrum of epoxy

© 2012 Wiley Periodicals, Inc.

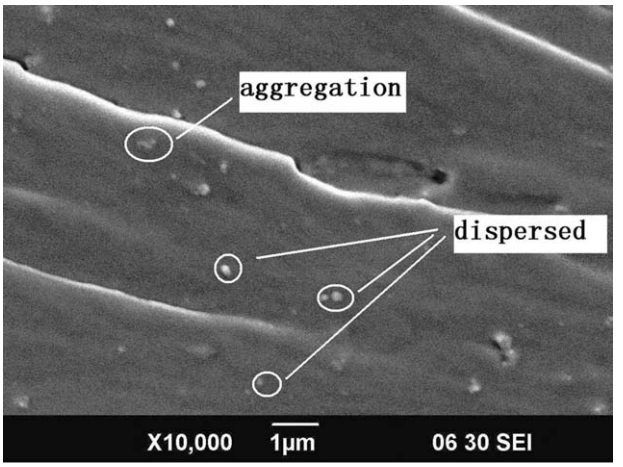

Figure 1. SEM image of the nanocomposite (5% loading by weight).

nanocomposites changed if it absorbed water. They concluded that the extra water was located around the surface of the nanoparticles and developed a water shell model to explain the results. Maity et al.[16] compared the spectra of EP containing different treatments nano-Al_2O_3 and considered that not only the presence of filler particles but also the nature of the interface affects the dielectric properties. They also found that adding silane-functionalized nano-Al_2O_3 decreases the real and imaginary parts of the nanocomposite dielectric constant and concluded that it is possibly affected by the covalent bonding of particles at the interfaces. Smaoui et al.[17] investigated dielectric relaxation spectroscopy and thermally stimulated currents in EP filled with nanoconductive particles. The interfacial relaxation and space charge density were found to be strongly dependent on the presence of nanofiller particles in epoxy nanocomposites.

Fothergill et al.[18–21] analyzed nanocomposite dielectric spectra in low frequencies and found them to be meaningful to the studies of space charge, aging, moisture content, as well as the electrical and mechanical properties of the material. However, the influence of nanofillers or interface on nanocomposite dielectric properties is not very clear, and analyses of dielectric spectra using Jonscher's Universal Relaxation Law (URL) are very few.

The URL developed by Jonscher considers the interaction of dipoles. Strong interactions between nanoparticles and a polymer in a nanocomposite may cause certain changes in dielectric spectra. Some useful results may be obtained if analyzed using the URL. In addition, some dielectric responses, especially phenomenon in low frequencies mentioned in literatures cannot be explained by the Debye theory. Therefore, this article applies this law to study the dielectric spectra of a polymer with different nanofiller loadings and to explain measurement results using a physical model.

Considering the fact that zinc oxide (ZnO) is an important wide band-gap semiconducting material with a potential for different applications,[22,23] we selected ZnO nanoparticles as fillers to be added to polymers. On the other hand, EP is a common insulation material in electrical apparatuses. Therefore, ZnO and EP were chosen as the main experiment materials in this research.

EXPERIMENTAL

All materials used in this study were commercially obtained. Bisphenol A-type liquid EP (type WSR618; epoxy index = 0.48–0.54) was supplied by the Bluestar New Chemical Materials Co., Wuxi Resin Factory, Jiangsu, China. The curing agent, methyl hexahydrophthalic anhydride, was analytically pure and was supplied by the Zhejiang Orient Chemical Plant, Jiaxing, China. The accelerating agent, dimethyl benzyl amine, was analytically pure and was supplied by the South Organic Chemical Co., Yancheng, Jiangsu Province, China. The nano-ZnO filler (average particle size = 20 nm; type HTZn-03; treated by aminopropyltriethoxysilane, a kind of silane coupling agent named KH550 in China) was supplied by Nanjing High Technology Nano Material Co., Jiangsu, China.

Nanoparticles tend to agglomerate in polymer matrices, which compromise the unique nanoparticle properties in the polymer. Therefore, two procedures, namely high shear mix and ultrasonic agitation, were used to disperse nanoparticles in preparing the epoxy nanocomposites. For the sample preparation, the required amount of nanoparticles was placed in a beaker and EP was added. Acetone was used to dilute epoxy, and the mixture was stirred for 30 min to preliminarily disperse the nanoparticles using a high-shear mechanical mixer (model T25; IKA Company, Staufen, Germany) at a speed of 10,000 rpm. Subsequently, the nanofillers were further dispersed for 30 min using an ultrasonic machine (model BILON-650Y; Shanghai Bilon Instruments Co., Shanghai, China). After the total evaporation of acetone from the beaker was ensured, fixed percentages of curing and accelerating agents (EP : curing agent : accelerating agent weight ratio = 100 : 90 : 2) were added. The mixture was stirred well and was degassed in a vacuum for about 0.5 h at 50°C. Finally, the fluid was cast in a plate mold and was oven-cured at 120°C for 8 h. After natural cooling to room temperature, the sample was collected to be measured.

The nanoparticle dispersion in the polymer was observed by scanning electron microscopy (SEM) (JSM-6390A). The glass transition temperature (T_g) of the nanocomposite was measured by differential scanning calorimetry (DSC) at heating rate of 10°C/min. The DSC instrument used was model DSC822e (METTLE TOLEDO, Langacher, Switzerland). Dielectric spectra were obtained using the Novocontrol Concept 80 (Hundsangen, Germany). The round test sample (diameter = 30 mm, thickness = 1 mm) was evaporated in a vacuum at the center of both sides of a 20-mm-diameter round gold electrode. The conditions were 1 V voltage, 20–160°C, and 10^{-1} to 10^6 Hz.

Table I. T_g of Epoxy Nanocomposite with Different Filler Loadings

Loading (wt %)	0	0.1	0.5	1	3	5
T_g (°C)	116.4	119.2	119.5	116.9	116.4	115.6

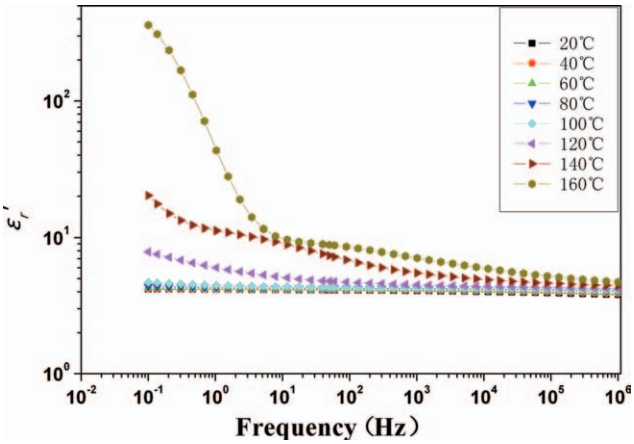

Figure 2. Spectra of ε_r' at different temperatures. [Color figure can be viewed in the online issue, which is available at wileyonlinelibrary.com.]

DISPERSION AND GLASS TRANSITION TEMPERATURE

A clamp was used to cut the round nanocomposite sample with 5 wt % nano-ZnO filler, which was then sprayed with gold on the cross-section. The cross-section image was observed by SEM (Figure 1).

Figure 1 shows that only a small amount of nanofillers were aggregated. Most of the nanofillers existed as single particles. This finding indicated that this method results in well-dispersed nano-ZnO fillers in epoxy.

T_g of the EP is closely related with its properties. Hence, T_g of the nanocomposite with different loadings was measured by DSC.

Table I shows that T_g of the EP is 116.4°C and that adding nano-ZnO fillers nearly had no effect on T_g of the nanocomposite.

DIELECTRIC SPECTRUM

Given that polymer polarization is related to frequency and temperature, obtaining the dielectric spectra of epoxy-ZnO nanocomposites at suitable temperature and frequency ranges is necessary.

Low-Frequency Dispersion

The dielectric spectra for the real and imaginary relative permittivities of EP from 20°C to 160°C are shown in Figures 2 and 3, respectively. Both are double logarithmic coordinate diagrams.

Figure 2 shows that at room temperature, the real relative permittivity ε_r' nearly had no relation with the frequency of the applied field. As frequency increased from 10^{-1} to 10^6, ε_r' changed very slightly (from 4.20 to 3.81), and the peak of the imaginary relative permittivity ε_r'' did not appear. At 120°C, which is higher than T_g of the EP, ε_r' rapidly increased with decreased frequency in a low frequency range. At 160°C, this phenomenon was more obvious, and ε_r' continually increased with decreased frequency in a full frequency range. There was an obvious turning frequency point at both sides wherein the change in ε_r' was linearly, but the slope of the line was smaller above this frequency than under. Still at 160°C, ε_r'' also had a turning frequency point, and the changes in ε_r'' were linearly both above and under this point. The conventional Debye relaxation theory, which states that dielectric loss peaks in a relaxation area, cannot explain the increase in both ε_r' and ε_r'' with decreased frequency and fact that there is no peak for ε_r''. This is the typical "low-frequency dispersion" (LFD)[24] phenomenon, which is a type of dielectric behavior in the URL.

The Debye theory has long been used to analyze dielectric fields, and it has succeeded in explaining the dielectric response of many systems. Jonscher[24,25] applied different points of view to explain dielectric relaxation. He found that materials have similar dielectric response properties despite the differences in their structures, chemical bonds, as well as physical and chemical properties, and he summed up an universal dielectric response theory named URL. The main difference between the Debye theory and the URL is the model they apply. The former applies a single model without considering the interactions (e.g., dipoles can shift unrestricted by others). The latter adopts an interactive multibody universal model, in which the shift of each dipole can affect that of other dipoles, while shift of others can affect shift of this dipole again. In addition, dipole shift or carrier movement is considered as a sudden and discontinued process in the URL. In a sense, we can say that the Debye theory is a special application of the URL under certain conditions. However, up to now, the universal dielectric theory has no clear physical model to quantificationally explain all dielectric behaviors.

In URL, the complex susceptibility $\tilde{\chi}$ is used to describe the dielectric response:

$$\tilde{\chi}(\omega) = \chi'(\omega) - i\chi''(\omega) = (\tilde{\varepsilon}(\omega) - \varepsilon_\infty)/\varepsilon_0. \quad (1)$$

$\chi'(\omega)$ and $\chi''(\omega)$ represent the rate and relaxation of susceptibility, respectively. $\tilde{\varepsilon}(\omega)$ is the complex dielectric permittivity, ε_∞ is the permittivity when the frequency is much higher than the frequency loss peak, and ε_0 is the permittivity of free space.

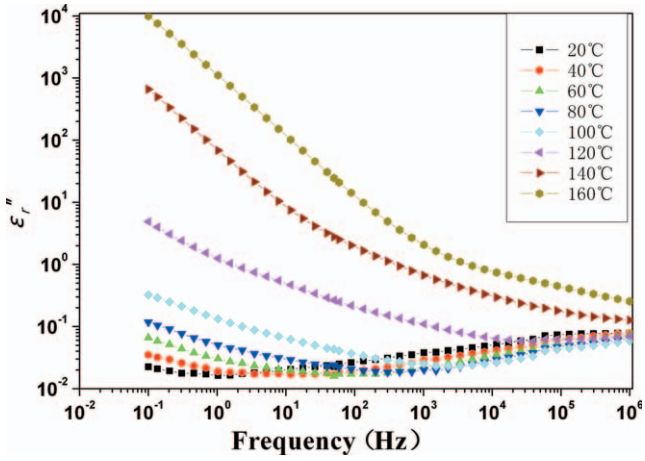

Figure 3. Spectra of ε_r'' at different temperatures. [Color figure can be viewed in the online issue, which is available at wileyonlinelibrary.com.]

Applied Polymer SCIENCE

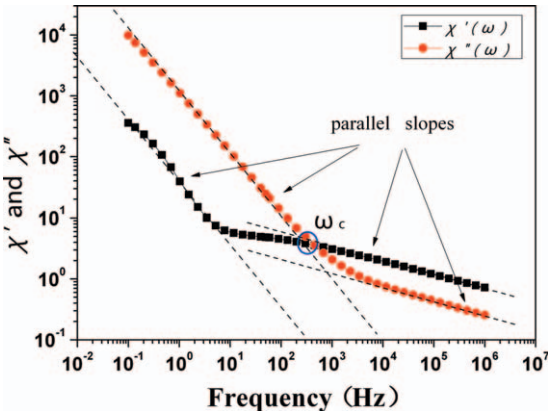

Figure 4. Spectra of $\chi'(\omega)$ and $\chi''(\omega)$ at 160°C. [Color figure can be viewed in the online issue, which is available at wileyonlinelibrary.com.]

According to the URL, all dielectric systems obey the universal law above the loss peak frequency ω_p:

$$\chi'(\omega) \propto \chi''(\omega) \propto \omega^{n-1}, \quad 1 > n > 0. \tag{2}$$

Equation (2) accompanies the consequence that the real and imaginary parts of the susceptibility are in the frequency-independent ratio described by:

$$\chi''(\omega)/\chi'(\omega) = \cot(n\pi/2), \tag{3}$$

which has the very simple physical significance that the ratio of

$$\frac{\text{energy lost per radian}}{\text{energy stored}} = \cot(n\pi/2). \tag{4}$$

To some materials, eq. (2) is obeyed in both the high- and low-frequency limits with the appropriate value of the index n:

$$\chi'(\omega) \propto \chi''(\omega) \propto \omega^{n_h-1} \quad 1 > n_h > 0 \quad \omega > \omega_c \tag{5}$$

$$\chi'(\omega) \propto \chi''(\omega) \propto \omega^{n_l-1} \quad 1 > n_l > 0 \quad \omega < \omega_c \tag{6}$$

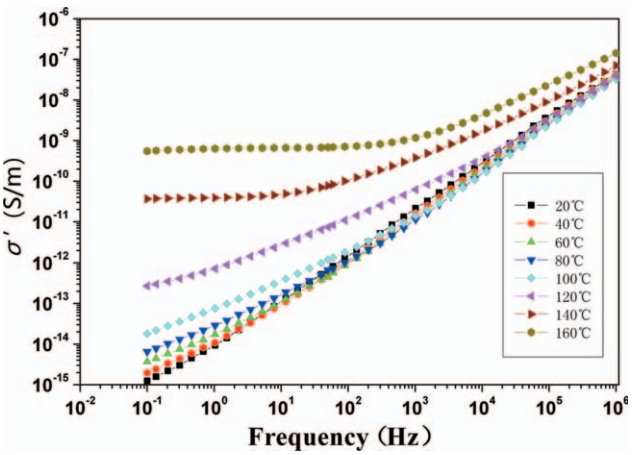

Figure 5. Spectra of σ' at different temperatures. [Color figure can be viewed in the online issue, which is available at wileyonlinelibrary.com.]

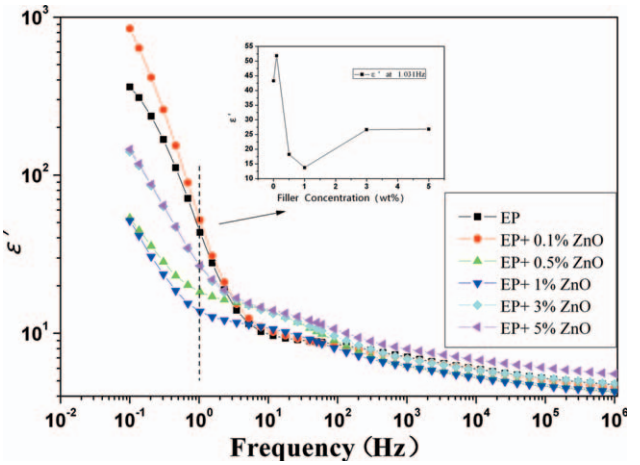

Figure 6. Spectra of ε_r' at different filler loadings. [Color figure can be viewed in the online issue, which is available at wileyonlinelibrary.com.]

ω_c is a characteristic frequency at both sides of which the $lg\chi'(\omega)$ and $lg\chi''(\omega)$ are parallel lines. n_h and n_l correspond to n in eq. (2) in high and low frequencies, respectively.

In fact, the relation among ε_r', ε_r'', $\chi'(\omega)$, and $\chi''(\omega)$ can be expressed as follows:

$$\chi'(\omega) = (\varepsilon'(\omega) - \varepsilon_\infty)/\varepsilon_0 = \varepsilon_r' - \varepsilon_\infty/\varepsilon_0 \tag{7}$$

$$\chi''(\omega) = \varepsilon''(\omega)/\varepsilon_0 = \varepsilon_r'' \tag{8}$$

Based on the results of this study, ε_∞ of the EP at 160°C is $4\varepsilon_0$. The values of $\chi'(\omega)$ and $\chi''(\omega)$ at 160°C were then be calculated, and their spectra are displayed in Figure 4.

$lg\chi'(\omega)$ and $lg\chi''(\omega)$ are clearly parallel straight lines outside a certain range of the frequency ω_c (about 450 Hz in Figure 6), which is the frequency of the intersection point. This result is consistent with the phenomenon described by the URL.

The spectra of the real conductivity σ' for epoxy at different temperatures is shown in Figure 5.

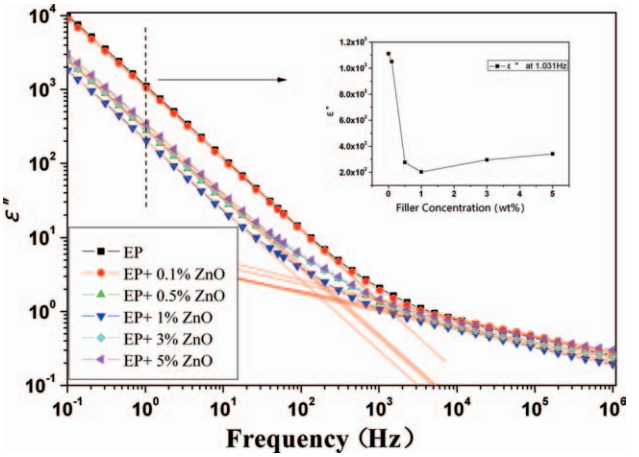

Figure 7. Spectra of ε_r'' at different filler loadings. [Color figure can be viewed in the online issue, which is available at wileyonlinelibrary.com.]

Table II. The Values of n at Low and High Frequencies

Loading wt %	0	0.1	0.5	1	3	5
Slope in low frequency	−0.968	−0.960	−0.939	−0.948	−0.935	−0.948
n_l	0.032	0.040	0.061	0.052	0.065	0.052
Slope in high frequency	−0.260	−0.236	−0.235	−0.241	−0.226	−0.205
n_h	0.740	0.764	0.765	0.759	0.774	0.795

Some changes occurred at the spectrum curve of σ' with temperature increase. At 160°C, conductivity strongly depended on frequency at frequencies higher than 10^4 Hz. At low frequencies, conductivity had little to do with frequency and was approximately constant. These results are similar with that of direct current conduction; hence, LFD is also called quasi-dc (QDC) behavior.[26] In fact, QDC is essentially different with the direct current. QDC related with polarization is a complex re-equilibrium process of the space charge under the outside field, including the transition, migration, trapping, and even electrochemical process. In contrast, direct current is related with the movement of carriers between electrodes.

The aforementioned phenomenon can also be found in the present epoxy-ZnO nanocomposites. Therefore, some instructive phenomena that deserves to be studied occurred in the nanocomposites at high temperatures. The next section discussed the measurement results at 160°C unless otherwise indicated.

Effect of the Incorporation of Nanofillers

The dielectric spectra of epoxy-ZnO nanocomposites with different filler loadings (at least three samples at each filler loading) were measured, and the median value of test results of each filler loading were taken to compare. Figures 6 and 7 show the spectra of ε_r' and ε_r'' of the nanocomposites, respectively.

Figures 6 and 7 show that at low frequencies, both ε_r' and ε_r'' decreased after nanofiller addition. ε_r' and ε_r'' both changed with increased nanofiller concentration at 1.031 Hz (shown as the small figure in Figures 6 and 7, respectively). The linearly fitted lines of ε_r'' at both low and high frequencies are also shown in Figure 7. According to eqs. (5) and (6), n_l and n_h listed in Table II was then calculated. The curves of n_l and n_h versus filler loadings are plotted in Figure 8. The error bars in Figure 8 refer to the maximum absolute deviation between median value and other values.

It should to be noted that the other way to find "n" is to use eq. (3). If the value of ε_∞ was estimated properly, the values of n acquired from two methods should be comparable, which further proved that the URL is appropriate and can be used to analyze the spectra of epoxy-ZnO nanocomposites. However, the exact value of ε_∞ is unknown, and it can be seen that ε_r' is not so smooth as ε_r'' from Figures 6 and 7, so the value of n obtained from the slope of ε_r'', which is taken to discuss in this article, should be more accurate and convincing.

Figure 8 shows that n_l and n_h all increased with increased nanofiller loading. n (including n_l and n_h) is related to the dielectric loss according to eq. (4). A greater n value corresponds to a lower dielectric loss change per radian.[24] Consequently, with increased nanofiller loading, changes in the dielectric losses of nanocomposites gradually decreased in a cycle.

Low-frequency dielectric loss can be more clearly understood by analyzing the nanocomposite conduction. In fact, between σ' and ε_r'', there exists the equation $\sigma' = \omega\varepsilon_0\varepsilon_r''$. σ' of epoxy-ZnO nanocomposites is shown in Figure 9. The small figure in Figure 9 shows that σ' changed with increased nanofiller concentration at 1.031 Hz.

QDC was found to decrease after nanofiller addition. Small nanofiller amounts such as 0.1 wt % had little effect on the material QDC. At 0.5 wt % concentration, QDC significantly

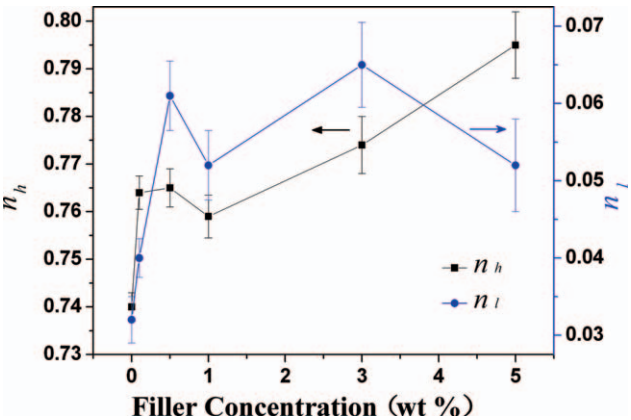

Figure 8. The values of n at low and high frequencies. [Color figure can be viewed in the online issue, which is available at wileyonlinelibrary.com.]

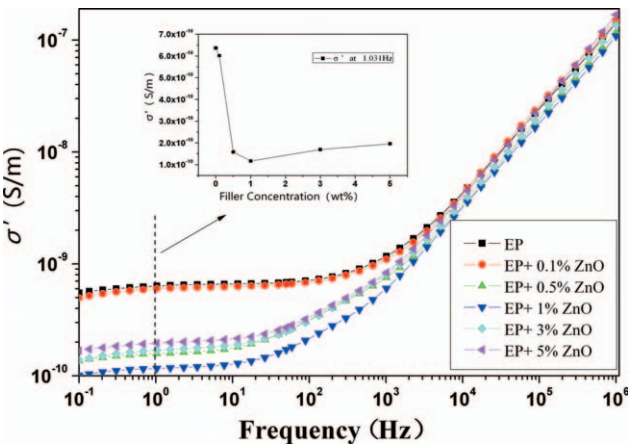

Figure 9. Spectra of σ' at different filler loadings. [Color figure can be viewed in the online issue, which is available at wileyonlinelibrary.com.]

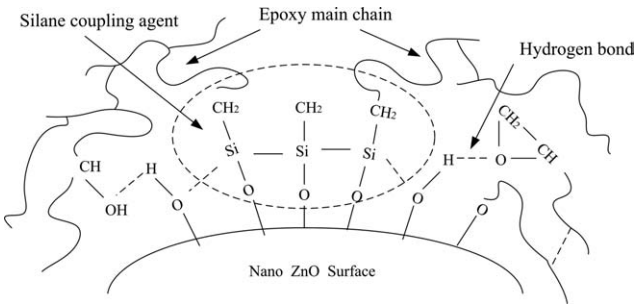

Figure 10. Schema of chemical bonding at the nanoparticle surface.

changed. Furthermore, increased nanofiller amounts had little effect on the QDC (Figure 9). However, several specimens abided by the same law in frequencies higher than 1000 Hz in this study. At the point where a lower QDC indicated lower gross dielectric losses of the nanocomposite, QDC seemed to have a similar function with the direct current.

Analysis

Below the glass transition temperature T_g, the molecular chain of the epoxy-ZnO nanocomposites has been "frozen." The dipole interaction can then be omitted, and the Debye theory can explain the phenomenon in the dielectric spectra of the nanocomposites. However, at high temperatures above T_g, the movement of the molecular chain strengthens, and the dipole interaction becomes obvious. Therefore, the Debye theory is no more suitable for interpreting some phenomena in dielectric spectra, such as LFD. However, these phenomena can be explained and analyzed by the URL, as aforementioned.

Both the dielectric constant and dielectric loss of ZnO, a semiconductor with $\varepsilon_r > 4.5$, are higher than those of epoxy. The dielectric constant and dielectric loss of epoxy-ZnO nanocomposites are decreased at high temperatures compared with those of pure epoxy. Hence, these changes may be related to the interface between nanoparticles and the epoxy matrix rather than to the nanoparticles themselves. Then, the possible reasons for the experiment results are analyzed by studying the structure of the interface. The LFD phenomenon is first explained.

Dissado and Hill[26] proposed a "cluster" model to explain the LFD phenomenon. They considered a material that has a regular structure in a small area and called it a "cluster." Intercluster charges and discharges form the polarization at a high frequency. Long charging and discharging times are considered as carrier transfer between clusters, which forms the QDC at a low frequency. However, this model seems inappropriate for discussing the relaxation behavior of amorphous polymers. Schonhals and Schlosser[27] suggested a model for amorphous polymers based on the idea that the molecular mobility at the glass transition is controlled by intra- and intermolecular interactions. At high frequencies, the polarization may primarily relate to the local movement of some chain units. At low frequencies, the polarization may be determined by the intermolecular correlation of the segments of different chains. This finding indicates that intermolecular correlation dominates the LFD phenomenon. The molecular movements are temperature dependent; thus, the LFD is closely related to the temperature.

Epoxy nanocomposites are an amorphous polymer, and Low-frequency dispersion section indicates that LFD is temperature-dependent. Therefore, the latter model is more suitable for epoxy nanocomposite. According to the model, the spectra of ε_r'' can be deduced to be related to the molecular mobility at both high and low frequencies. Moreover, n_h may also be concerned with the movement of local chains, whereas n_l may depend on the intermolecular correlation. The decrease in the dielectric loss implied that the movement of some polymer molecule chains were restrained because of the nanofiller addition. Despite the lack of direct experimental evidence, an attempt is made to describe the interface, as follows.

Nano-ZnO particle surfaces treated with the silane coupling agent kH550 are partly occupied by hydroxyl groups and are partly grafted by the coupling agent. Hence, part of the filler surface connected with the epoxy matrix through hydrogen bonding, and other parts linked via the coupling agent (Figure 10). Subsequently, a bonded region is formed at interface to tightly connect two materials. The actual composition of a Epoxy-ZnO nanocomposite may be schematically diagrammed as Figure 11. Therefore, the addition of nanoparticles generally enhanced the molecular interactions within the EP.

At a high temperature and a low frequency, the nanocomposite permittivity decreases after nanoparticle addition partly because there is no interfacial polarization,[16] and partly because the movement of some polymer chains is restrained by chemical bonds at the interface. In turn, decreased nanocomposite permittivity shows the nanofillers is closely combined with EP.

In addition, strong interactions around nanofillers may induce the changes in n. The strong bonding may limit not only part of the local chain movement but also some relative molecule movements. Therefore, n, both in high and low frequencies, which is associated with the molecular mobility has been affected. The addition of nanoparticles to EP results in increased n, or rather, in decreased dielectric losses in a cycle.

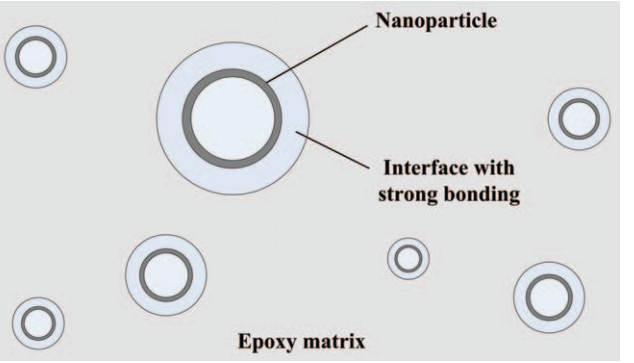

Figure 11. Diagram of nanoparticle distribution within the epoxy matrix. [Color figure can be viewed in the online issue, which is available at wileyonlinelibrary.com.]

Given that a clear theoretical URL model for explaining dielectric responses still does not exist, the impact of nanofillers on epoxy can only be discussed qualitatively. However, from the measurements in this study, we have proven that the interface with strong bonding between nanoparticles and the epoxy matrix is important to determine the nanocomposite dielectric properties.

CONCLUSIONS

In this article, the spectra of Epoxy-ZnO nanocomposites with different loadings were obtained. The results were analyzed using the URL, and the dielectric spectra at 160°C were especially compared. The following conclusions are drawn.

1. For the nanocomposite prepared in the present experiments, LFD does not occur until the temperature is higher than T_g. The phenomenon is very typical at 160°C.
2. At high temperatures after nanofiller addition, the real relative permittivity ε_r' of the nanocomposite decreases at low frequencies. For the imaginary relative permittivity ε_r'', the value of n (calculated from the ε_r'' spectra of the nanocomposites) increases both at high and low frequencies. In other words, changes in the dielectric loss decreases in a cyclical manner with increased nanofiller loading. The decrease in the gross dielectric loss at low frequencies is better explained using the QDC of the nanocomposite.
3. If nanofillers are well dispersed in epoxy, an interface with strong bonding can be built between two materials, and strong bonding may restrain the movement of some molecule segments and chain units, and then lead to increased n_l and n_h, which is calculated from the ε_r'' spectra.

The dielectric spectra of EP undergo delicate changes on nanofiller addition. Analyzing the changes in the nanocomposite dielectric properties using the URL is helpful in understanding the mechanisms of nanofillers affecting a polymer. Knowing the nanoeffect of the fillers in a polymer could also be a basis for designing high-performance materials.

REFERENCES

1. Tanaka, T. *IEEE Trans. Dielectr. Electr. Insul.* **2005,** *12*, 914.
2. Li, S.; Yin, G.; Chen, G.; Zhong, L.; Zhang, Y.; Lei, Q. *IEEE Trans. Dielectr Electr. Insul.* **2010,** *17*, 1523.
3. Tanaka, T.; Montanari, G. C.; Mulhaupt, R. *IEEE Trans. Dielectr. Electr. Insul.* **2004,** *11*, 763.
4. Tuncer, E.; Sauers, I.; James, D. R.; Ellis, A. R.; Paranthaman, M. P.; Aytug, T.; Sathyamurthy, S.; More, K. L.; Li, J.; Goyal, A. *Nanotechnology* **2007,** *18*, 1.
5. Lewis, T. J. *IEEE Trans. Dielectr. Electr. Insul.* **1994,** *1*, 812.
6. Lewis, T. J. *IEEE Trans. Dielectr. Electr. Insul.* **2004,** *11*, 739.
7. Roy, M.; Nelson, J. K.; MacCrone, R. K.; Schadler, L. S.; Reed, C. W.; Keefe, R.; Zenger, W. *IEEE Trans. Dielectr. Electr. Insul.* **2005,** *12*, 1273.
8. Tanaka, T.; Kozako, M.; Fuse, N.; Ohki, Y. *IEEE Trans. Dielectr. Electr. Insul.* **2005,** *12*, 669.
9. Fothergill, J. C. IEEE International Conference on Solid Dielectrics, Winchester, UK, **2007,** pp 1–10.
10. Cao, Y.; Irwin, P. C.; Younsi, K. *IEEE Trans. Dielectr. Electr. Insul.* **2004,** *11*, 797.
11. Montanari, G. C.; Fabiani, D.; Palmieri, F. *IEEE Trans. Dielectr. Electr. Insul.* **2004,** *11*, 754.
12. Castellon, J.; Nguyen, H. N.; Agnel, S.; Toureille, A.; Frechette, M.; Savoie, S.; Krivda, A.; Schmidt, L.E. *IEEE Trans. Dielectr. Electr. Insul.* **2011,** *18*, 651.
13. Bánhegyi, G.; Hedvig, P.; Petrovićac, Z. S.; Karasz, F. E. *Polym.-Plast. Technol. Eng.* **1991,** *30*, 183.
14. Zhang, C.; Stevens, G. C. *IEEE Trans. Dielectr. Electr. Insul.* **2008,** *15*, 606.
15. Zou, C.; Fothergill, J. C.; Rowe, S. W. *IEEE Trans. Dielectr. Electr. Insul.* **2008,** *15*, 106.
16. Maity, P.; Poovamma, P. K.; Basu, S.; Parameswaran, V.; Gupta, N. *IEEE Trans. Dielectr. Electr. Insul.* **2009,** *16*, 1481.
17. Smaoui, H.; Lassad E. L. M.; Guermazi, H.; Agnel, S.; Toureille, A. *J. Alloys Compd.* **2009,** *477*, 316.
18. Nelson, J. K.; Fothergill, J. C.; Dissado, L. A.; Peasgood, W. 2002 Annual Report Conference on Electrical Insulation and Dielectric Phenomena, Cancun, Quintana Roo, Mexico, **2002,** p 295.
19. Fothergill, J. C.; See, K. B. A.; Ajour, M. N.; Dissado, L. A. Proceedings of 2005 International Symposium on Electrical Insulating Materials (ISEIM 2005), Kitakyushu, Japan, **2005,** p 821.
20. Ajour, M. N.; Dissado, L. A.; Fothergill, J. C.; Norman, P. N. Annual Report Conference on Electrical Insulation and Dielectric Phenomena, Cancun, Quintana Roo, Mexico, **2002,** p 438.
21. Fothergill, J. C.; Nelson, J. K.; Fu, M. Annual Report Conference on Electrical Insulation and Dielectric Phenomena, Boulder, Colorado, USA, **2004,** p 406.
22. Dang, Z. M.; Fan, L. Z.; Zhao, S. J.; Nan, C. W. *Mater. Res. Bull.* **2003,** *38*, 499.
23. Tjong, S. C.; Liang, G. D.; Bao, S. P. *J. Appl. Polym. Sci.* **2006,** *102*, 1436.
24. Jonscher, A. K. Universal Relaxation Law. Xi'an Jiaotong University Press: Xi'an, **2008.**
25. Jonscher, A. K. Dielectric Relaxation in Solids. Xi'an Jiaotong University Press: Xi'an, **2008.**
26. Dissado, L. A.; Hill, R. M. *J. Chem. Soc., Faraday Trans. 2* **1984,** *80*, 291.
27. Schonhals, A.; Schlosser, E. *Colloid Polym. Sci.* **1989,** *267*, 125.